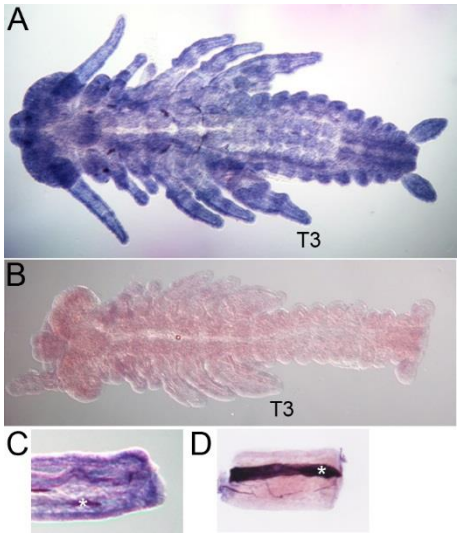


**Supplementary material Fig. 1. *Gb'E(z)* and *Gb'Utx* expression patterns.**
*Gb'E(z)* and *Gb'Utx* mRNA localisation in developing embryos and regenerating legs as shown by whole mount *in situ* hybridisation. (A-B) *Gb'E(z)* expression pattern in stage 10 embryos (A) and *Gb'Utx* expression in stage 9 embryos (B). (C-D) *Gb'E(z)* (C) and *Gb'Utx* (D) expression patterns in regenerating legs at 2 dpa. Asterisks indicate non-specific staining.

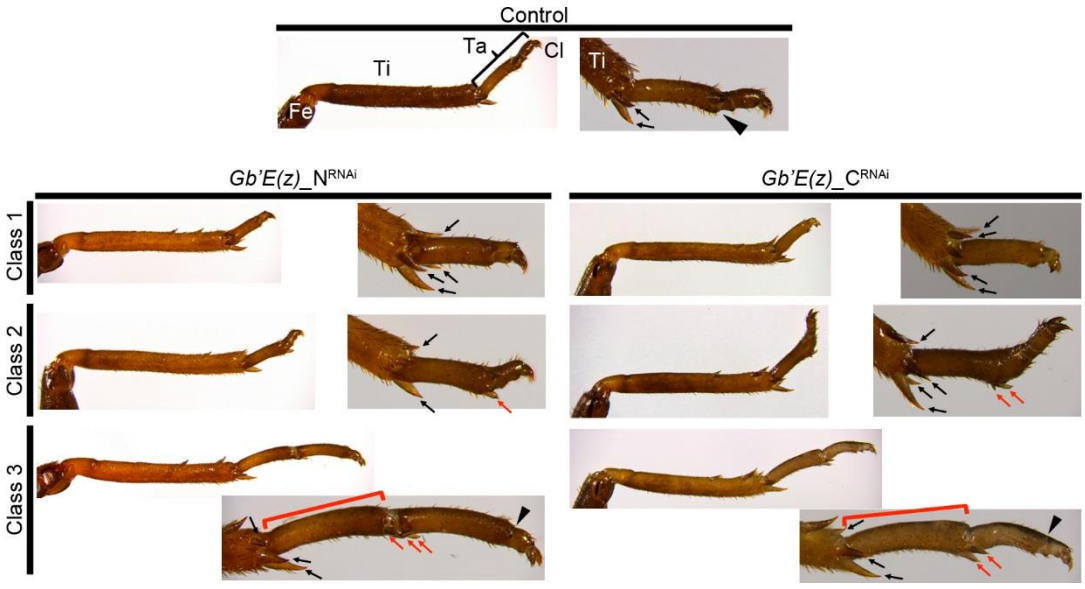


**Supplementary material Fig. 2. Confirmation of *Gb'E(z)*$^{RNAi}$ off-target effects.**
Typical regenerating legs of control and RNAi crickets against *Gb'E(z)*_N (left column) and *Gb'(z)*_C (right column) at sixth instar. Tibial spurs and tarsal spurs are indicated by arrows and arrowheads, respectively, and tibial spurs on extra tibia segments are indicated by red arrows. The extra tibia segments are indicated by brackets. Fe, femur; Ti, tibia; Ta, tarsus; Cl, claw.

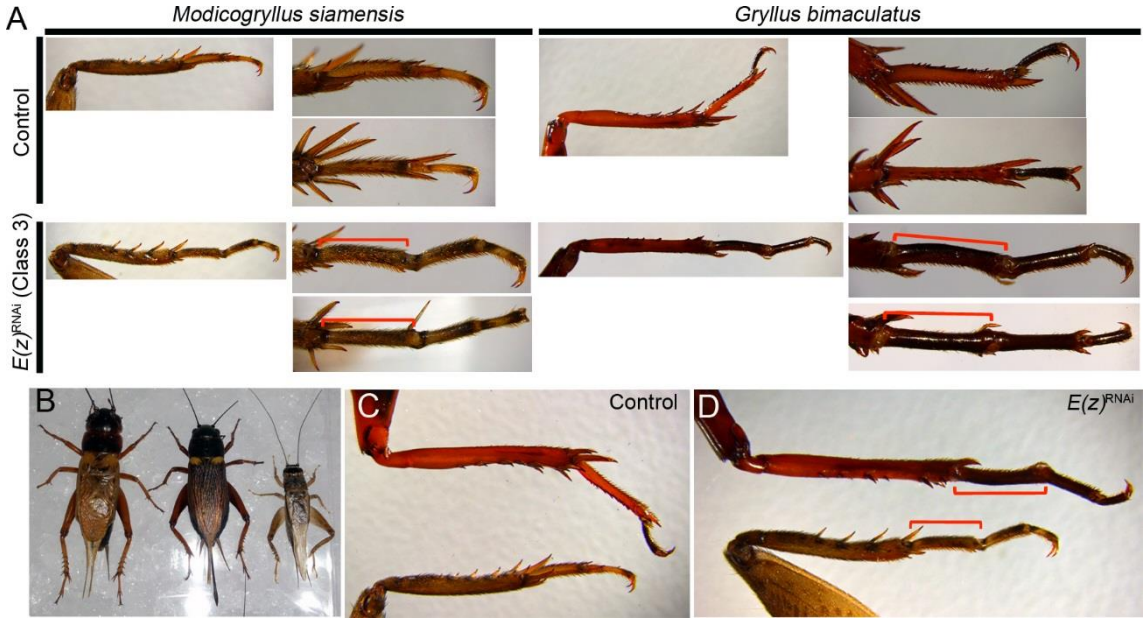


**Supplementary material Fig. 3. Regenerated *Gryllus bimaculatus* and *Modicogryllus siamensis* legs.**
(A) Typical phenotypes of control (upper panels) and *E(z)*$^{RNAi}$ (lower panels) regenerated legs of *Gryllus bimaculatus* (right column) and *Modicogryllus siamensis* (left column) are shown. Lateral views of low magnification images are shown in the left columns, and lateral and dorsal views of high magnification images are shown in the upper and lower sides in right columns. The extra tibia segments are indicated by red brackets. (B) Whole bodies of male and female *Gryllus bimaculatus* (left and middle) and male *Modicogryllus siamensis* (right). (C-D) Comparison of *Gryllus* (upper) and *Modicogryllus* (lower) regenerated legs of control (C) and *E(z)*$^{RNAi}$ crickets (D). The extra tibia segments are indicated by red brackets.

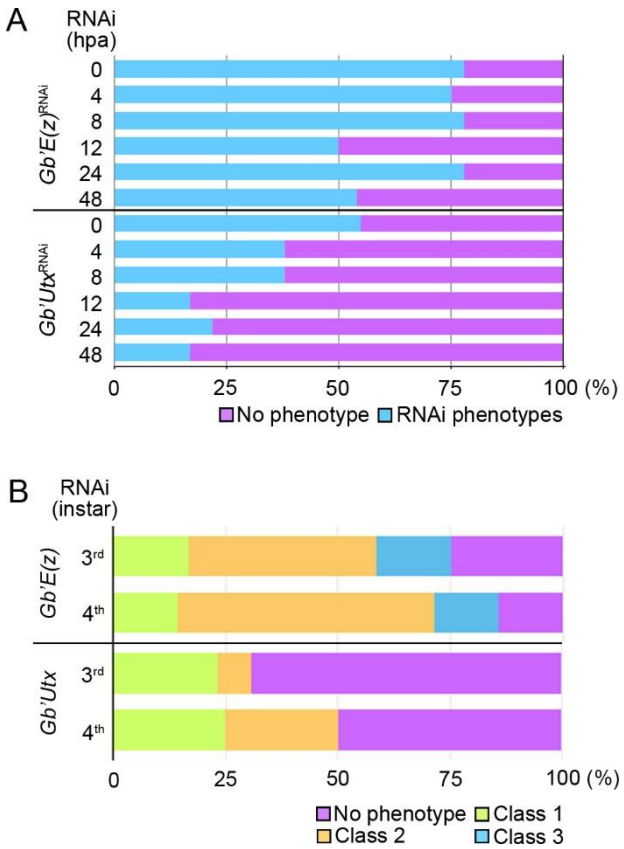


**Supplementary material Fig. 4. Penetrance of regenerated leg RNAi against epigenetic factors before amputation.**

(A) Graph shows the ratios (%) of abnormal regenerated legs (including phenotypes class 1, 2 and 3 of *Gb'E(z)*$^{RNAi}$ and phenotypes class 1 and 2 of *Gb'Utx*$^{RNAi}$) compared with normal regenerated legs at each time point. In this graph, "hpa" means incubation period (hours) from amputation to RNAi. (B) Graph shows ratio of RNAi phenotypes against *Gb'E(z)* and *Gb'Utx*. "3$^{rd}$ RNAi" denotes the phenotype ratio of regenerated legs with RNAi at third instar and amputated at fourth instar. "4$^{th}$ RNAi" denotes the phenotype ratio of regenerated legs with RNAi and immediately amputated at fourth instar.


**Supplementary material Fig. 5. Typical embryonic phenotypes in the control and *Gb'Utx*$^{RNAi}$ crickets.**
Lateral and dorsal views of control and *Gb'Utx*$^{RNAi}$ embryos at stage 13 are shown. *Gb'Utx*$^{RNAi}$ embryos exhibited abnormal morphologies in the head segments.

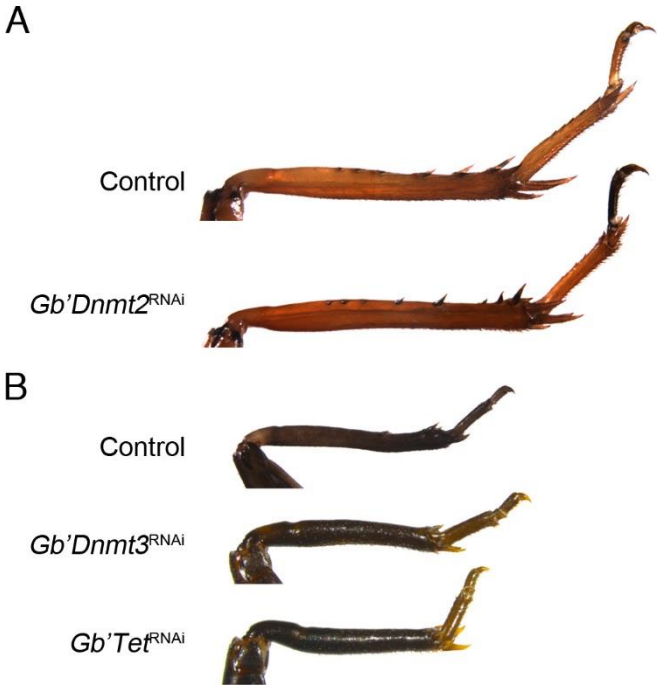


**Supplementary material Fig. 6. Typical regenerated leg phenotypes in the control, *Gb'Dnmt2*$^{RNAi}$, *Gb'Dnmt3*$^{RNAi}$ and *Gb'Tet*$^{RNAi}$ crickets.**
Lateral views of regenerated legs are shown. (A) Regenerated legs in the control and *Gb'Dnmt2*$^{RNAi}$ adults. (B) Regenerated legs in the control, *Gb'Dnmt3*$^{RNAi}$ and *Gb'Tet*$^{RNAi}$ at sixth instar nymphs.